The heart of oxygenic photosynthesis illuminated

Janssen, G.J.

Chapter 4

Photochemically induced dynamic nuclear polarization NMR on photosystem II obtained directly from plants reveals remarkable similarity and robustness of the radical pair across species.

The solid-state photo-CIDNP (photochemically induced dynamic nuclear polarization) effect allows for dramatic signal enhancement of the photochemically active machinery in solid-state magic-angle spinning (MAS) NMR spectroscopy. Here we present photo-CIDNP MAS NMR data from photosystem II of *Spirodela oligorrhiza* (duckweed), using biosynthetic sparse ^{13}C isotope labeling of PSII. Extending our earlier data collected from D1D2 preparations, it is shown that photo-CIDNP signals from selected ^{13}C nuclei within the heart of the large PSII protein can be obtained directly from entire plants, BBY, thylakoid membranes and core particles as well. Despite the presence of both PSI and PSII, the photo-CIDNP signals arise selectively from the PSII radical pair within the plants. The coherent evolution of the radical pair is enabled by a combination of blocking of electron transfer from the $P680^-$ to the Tyr_Z and the OEC and blocking or loss of the Q_A plastoquinone. The source of the photo-CIDNP response is remarkably robust, remains essentially unaffected by the various preparation procedures, and is similar for duckweed and *Spinacia oleracea* (spinach). Both in the electronic ground state and in the radical cation state the electronic structure of $P^+_{D1}Phe^-_{D1}$ is highly conserved between different plant species. The radical pair is formed by a single Chl *a* donor and a single Phe *a* acceptor. Thus, according to the photo-CIDNP the P^+_{680} donor, assigned to P^+_{D1}, is monomeric and only weakly coupled to the neighboring P_{D2}. In contrast, strong evidence for a matrix involvement, probably a histidine sidechain, in the radical pair is found.

4.1 INTRODUCTION

The photosynthetic machinery found in plants converts energy from the sun into chemical energy by oxidizing water and reducing carbon dioxide, while releasing oxygen as a side product. To achieve this, two large trans-membrane protein complexes, PSII and PSI, operate in tandem (for a review see *e.g.* Blankenship *et al.* 2002). While PSII has the highest oxidation power known in living nature, +1.2 V, PSI has the strongest reductive power (ca.-0.5 V) (Gorkom and Schelvis 1993; Witt 1996; Holzwarth *et al.* 2006; Nakamura *et al.* 2011). How PSII is able to produce and maintain such high potential within a 'soft' protein environment, has been the subject of extensive research by optical-kinetic (Hughes *et al.* 2010; Romero *et al.* 2010; Novoderezhkin *et al.* 2011) and magnetic resonance techniques (Kammel *et al.* 2003; Lendzian *et al.* 2003; Lubitz 2003; Diller *et al.* 2007). The strong oxidising nature of the cation of PSII has been attributed to a monomeric chlorophyll species that is in the right position within the large PSII multiprotein complex to experience a strong effect from the backbone dipoles of the trans-membrane helices (for a review see Cardona et *al.* 2012). Recently a high resolution X-ray structure, of a dimeric PSII core complex from cyanobacteria *Thermococcus vulcanus* has been resolved down to 1.9 Å resolution (Umena *et al.* 2011). The PSII reaction center, or D1D2 complex, consists of the D1 and D2 polypeptides in which two branches of cofactors are symmetrically arranged (Figure 4.1C). The cofactors consist of two inner Chlorphyll *a* (Chl *a*) molecules (P_{D1} and P_{D2}), two accessory Chl *a* (Chl $_{D1}$ and Chl $_{D2}$) two Pheophytins *a* (Phe *a*) and two quinones (Q) arranged in two symmetric branches. In addition the PSII RC contains two β-carotenes and two peripheral Chl *a* (Chl_{p1} and Chl_{p2}) (Figure 4.1C).

Excited state dynamics investigations have shown that the initial charge separation in oxygenic photosynthesis is provided by a multimer of four chlorophyll *a* (Chl_{D1}, P_{D1}, P_{D2}, Chl_{D2}) and two pheophytin *a* (Phe_{D1} and Phe_{D2}) pigments embedded in the PSII membrane protein complex (Kamlowski *et al.* 1996; Holzwarth *et al.* 2006; Raszewski *et al.* 2008; Novoderezhkin *et al.* 2011). Using the optical transition energies and the X-ray data as a basis, the energy levels of the various pigments were calculated. It was found that the energies of the components in the multimer are different, and that the energies of Chl_{D1} and P_{D1} depend on the temperature (Raszewski *et al.* 2008). At cryogenic temperatures the excited state is strongly localized on the accessory Chl_{D1}, while at physiological temperatures there are contributions from all chlorophyll pigments to the primary excited state (Raszewski *et al.* 2008). Charge separation is thought to involve at least two different pathways, with

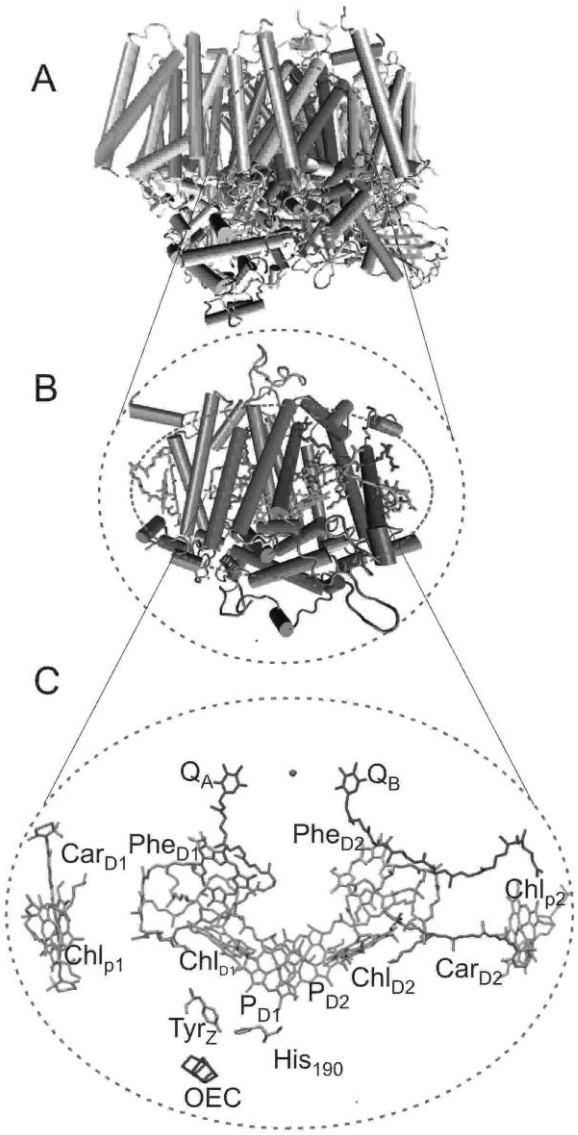

Figure 4.1: (A) PSII core complex. (B) D1D2 reaction center complex. (C) The arrangement of cofactors of electron transfer chain located in D1D2 complex consists of two central Chl *a* (P_{D1} and P_{D2}), two accessory Chl *a* (Chl_{D1} and Chl_{D2}), two pheophytins (Phe_{D1} and Phe_{D2}), two Quinone's (Q_A and Q_B), two peripheral Chl *a* (Chl_{p1} and $Chlp_2$) and two β-carotenoids (Car_{D2} and Car_{D1}). At the P_{D1} side a Tyrosine residue Tyr_Z is bridging between the P_{D1} and the Oxygen evolving system (OEC).

electron transfer from the Chl_{D1} to the Phe_{D1} or from the $P_{D1}P_{D2}$ excitonically coupled dimer to the Phe_{D1} (Raszewski *et al.* 2008; Novoderezhkin *et al.* 2011). Within ~20 ps the complex charge separation processes have occurred, and the hole stabilizes on P_{D1} to produce the $P^+_{D1}Phe^-_{D1}$ in its non-stationary correlated radical pair state (Raszewski *et al.* 2008).

The photo-CIDNP magic-angle spinning (MAS) NMR is an optical solid-state NMR method exploiting the coherent evolution in the spin-correlated electron pair. The conversion of electron spin zero quantum coherence into T_0 double quantum coherence by coupling to the nuclear spins leads to nuclear polarization and allows for a strong increase of sensitivity

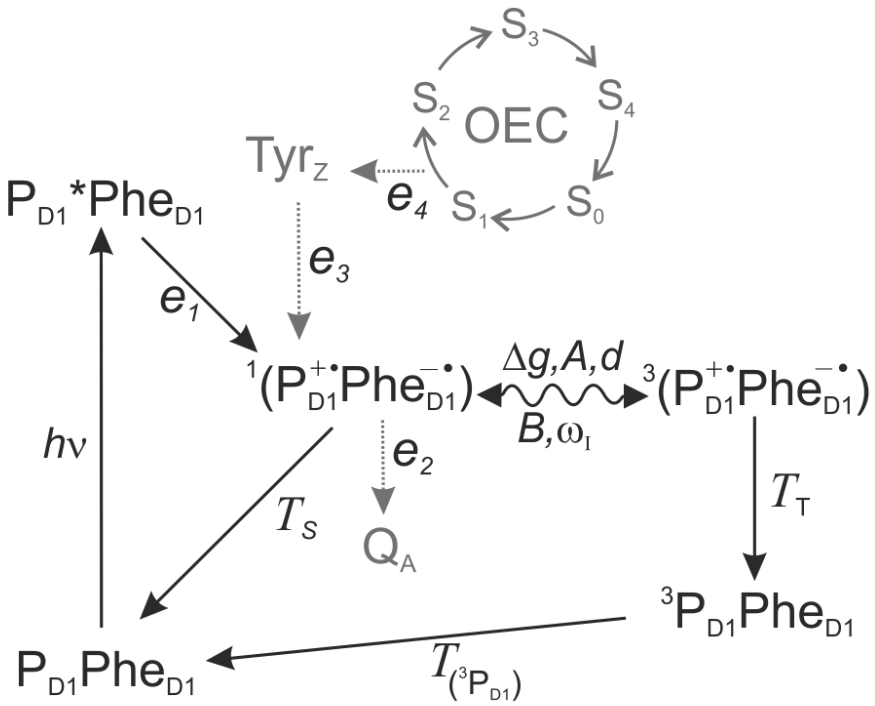

Figure 4.2: Reaction cycle in PSII D1D2 particles. After absorption of a photon ET occurs from the Chl donor P_{D1} to the primary acceptor Phe_{D1}. The oscillating arrow represents coherent evolution of the initial zero quantum coherence of the pure singlet state into double quantum coherence of the triplet radical pair and back. This process is driven by the difference of the *g* value between the two electrons Δg, the secular part of the hyperfine interaction *A*, the coupling between the two electrons *d*, the pseudo-secular hyperfine coupling *B*, and the nuclear Zeeman frequency ω_I. T_S, T_T and $T(^3P_{D1})$ refer to the lifetimes of the singlet and the triplet radical pairs, and the triplet donor state, respectively. The direction of the excitation and decay after light induced electron transfer from the electron donor (P_{D1}) to the Phe_{D1} acceptor, are shown in solid arrows. Depicted in grey are the S-cycle of the OEC, the Tyr_Z residue bridging between the OEC and the P_{D1} chlorophyll donor and the secondary electron acceptor Q_A. In PSII systems larger than D1D2 (*i.e.* the PSII core, BBY, thylakoid and plants) both the OEC and the Q_A are present and ET steps e_2 to e_4 cause fast quenching of the singlet radical pair $1(P_{D1}^{\bullet+}Phe_{D1}^{\bullet-})$ avoiding ISC and subsequent triplet state buildup.

and selectivity of NMR signals. This makes it possible to study the electronic structure of photosynthetic cofactors in great detail (Zysmilich and McDermott 1994; Jeschke and Matysik 2003; Daviso *et al.* 2009). The spin-chemical origin of the photo-CIDNP effect is based on the contribution of different mechanisms, TSM (Jeschke 1998), DD (Polenova and McDermott 1999) and DR (Zysmilich and McDermott 1994). While the observed chemical shift refers to the electronic ground state obtained after the photocycle, the photo-CIDNP intensity is related in a non-trivial manner to the local electron spin density in the radical pair state (Daviso *et al.* 2009). Until recently the solid-state photo-CIDNP effect has been observed only in natural photosynthetic RCs (Matysik *et al.* 2009). Observation of solid-state photo-CIDNP in a blue-light photoreceptor (Thamarath *et al.* 2010) as well as the prediction that it occurs at earth fields (Jeschke *et al.* 2011) suggest that the phenomenon is rather common in electron transfer systems.

Photo-CIDNP MAS NMR has been successfully applied to various photosynthetic RCs from bacteria and plants (Alia *et al.* 2004; Roy *et al.* 2007; Roy *et al.* 2008) and a strong increase in sensitivity and selectivity by the solid-state photo-CIDNP effect has been observed. In combination with selective isotope labeling the photo-CIDNP allows for direct observation of the primary radical pair in entire cells of selectively ^{13}C labeled purple bacteria (Prakash *et al.* 2003) and cyanobacteria *Synechocystis* sp. PCC 6803 (chapter 2; Janssen *et al.* 2010). In PSII the relatively stable $P_{D1}^{+}Phe_{D1}^{-}$ radical pair can contribute to photo-CIDNP via the TSM and DD mechanisms on the ns timescale, while charge recombination triplets that can possibly contribute to the photo-CIDNP via the DR mechanism are expected to equilibrate between Chl_{D1} and P_{D1} (Figure 4.2).

For PSII the Photo-CIDNP effect has been detected for D1D2 preparations only (Matysik *et al.* 2000; Diller *et al.* 2005). Based on the PSII photo-CIDNP data, the donor was identified to be a single Chl *a* cofactor with little interaction with other pigments (Matysik 2000; Diller *et al.* 2005). This is in line with theoretical studies (Durrant *et al.* 1990; Raszewski *et al.* 2008) and ADMR experiments (van der Vos *et al.* 1992) concluding the P_{D1} donor to be only weakly coupled to the neighboring P_{D2} and functioning as a monomer. It has been proposed that the high oxidation power of PSII, +1.2 V, relative to the closely related RC of purple bacteria, + 0.7 to 0.9 V, may be due to the localization of the cation on a single Chl *a* pigment rather than being distributed over a strongly coupled bacterial chlorophyll (BChl) pair (Groot *et al.* 2005; Holzwarth *et al.* 2006; Saito *et al.* 2011). Photo-CIDNP data also reveal a pronounced asymmetry of the electronic spin density (ρ_i) distribution within the Chl *a* donor (Käss *et al.* 1995; Matysik 2000; Diller *et al.* 2005). The pattern of electron spin density distribution was found to be inverted in the oxidized radical state relative to Chl $a^{+\bullet}$ in solution with a much lower redox potential of -0.5 V compared to the Chl *a* donor inside the PSII RC. While monomeric Chl *a* in solution has the highest ρ_i located at ring II (Käss *et al.* 1995), the Chl *a* cation radical in the D1D2 complex shows a shift of ρ_i towards ring III and IV (Matysik 2000; Diller *et al.* 2005; Diller *et al.* 2007). A possible explanation of the ρ_i inversion was suggested to be the presence of a local electrostatic field close to ring III, illustrated in a computational model by the protonation of the keto group of ring IV (Matysik 2000). However improved assignment of ^{13}C resonances of Chl *a* is still demanding for confirming the source of ρ_i sign inversion. Based on data obtained from uniformly ^{15}N labeled D1D2, the inversion of electron spin density observed in the oxidized radical state of the Chl *a* donor was proposed to originate from a tilting of the

axial histidine toward pyrrole ring IV causing π-π overlap of both aromatic systems (Diller *et al.* 2005).

Until now photo-CIDNP MAS NMR studies on plant PSII have been restricted to experiments on isolated D1D2, which is prepared following a harsh biochemical procedure (Matysik 2000; Diller *et al.* 2005). First thylakoid membrane containing PSI and PSII are isolated and then PSI is removed to obtain PSII enriched membranes (so-called BBY preparations) (Novoderezhkin *et al.* 2011). Next the removal of peripheral light harvesting complex 2 (LHC2) leads to PSII core complex (van Leeuwen *et al.* 1991). Finally removal of core antenna proteins CP43 and CP47 leads to the PSII reaction center or D1D2 complex (Figure 4.1B).

The question arises whether the electronic structure of the non-stationary correlated radical pair state ($P^{+}_{D1}Phe^{-}_{D1}$) is influenced in isolated D1D2 complex as compared to intact RC in PSII core or in higher preparations. Previously a novel application of photo-CIDNP MAS NMR has been recognized where the radical pair in the photosynthetic bacterial reaction center was studied directly in intact cells (Prakash *et al.* 2003). However, Photo-CIDNP buildup in large PSII systems (*i.e.* PSII core complex, BBY complex or thylakoid membrane) is challenging because of sensitivity issues and previous attempts of ^{13}C isotope labeling of PSII in plants have not been successful. In addition, the presence of quinones and the oxygen evolving complex, which cause fast quenching of the singlet radical pair avoiding intersystem crossing (ISC) and subsequent triplet state buildup, will cause additional problems for Photo-CIDNP buildup in larger PSII systems (Figure 4.2). In order to observe photo-CIDNP, the nonstationary singlet state that is generated by photoexcitation and charge separation, $P^{+}_{D1}Phe^{-}_{D1,}$ has to evolve coherently for ~ 10-100 ns. An essential difference between higher PSII preparations on the one hand, and D1D2 or bacterial RCs on the other hand, is the presence of an "upstream" depletion mechanism by hole transfer from the radical cation P^{+}_{D1} to the Tyr_Z and the OEC, in addition to the "downstream" depletion from electron transfer from the Phe^{-}_{D1} to the quinone acceptor (Figure 4.2). Thus, in order to observe photo-CIDNP in higher PSII preparations, the removal or blocking by intense illumination of quinones that was successfully exploited in photo-CIDNP studies of the D1D2 and bacterial RC preparations to block the downstream transfer is insufficient.

In this work we successfully incorporate selective ^{13}C labels in PSII of duckweed and report photo-CIDNP signals of PSII directly from core particles, thylakoid membranes and entire plants. The coherent evolution of the radical pair is enabled by a combination of pH-

induced blocking of electron transfer from the $P680^-$ to the Tyr_Z and the OEC and blocking or loss of the Q_A plastoquinone. Despite the presence of both PSI and PSII, the photo-CIDNP signals arise selectively from the PSII radical pair within the plants. The electronic structure of $P^+_{D1}Phe^-_{D1}$ is presented and compared at various steps of PSII isolation, from the entire plant to the D1D2 complex. The results show that the photochemical machinery of PSII is remarkably robust and that the electronic structure of the non-stationary correlated radical pair state, the source of the photo-CIDNP response, remains essentially unaffected by the various preparation procedures. Finally the data reveal and contribute to converging evidence that the P^+_{680} donor is, also at higher temperature, P^+_{D1}, and only loosely coupled to the neighboring P_{D2} functioning as a monomer.

4.2 MATERIALS AND METHODS

4.2.1 Strains and culture conditions

Duckweed plants were grown under aseptic conditions on half-strength Hunter's medium (Posner 1967) under continuous light (20 $\mu Em^{-2}s^{-1}$) at 25 °C. The medium was continuously bubbled with sterile air containing 5% CO_2. For selective ^{13}C labeling fully grown plants were exposed to δ-aminolevulinic acid (ALA, purchased from Cambridge Isotope Laboratories), isotopically ^{13}C labeled at carbon position 3, (3-ALA), 4, (4-ALA) or 5, (5-ALA), to a final concentration of 1.4 mM in half-strength Hunter's medium at pH 4.8. After 7 day's plants were harvested and used directly for sample preparation or frozen in liquid nitrogen and stored at -80 °C until further use.

4.2.2 Determination of the ^{13}C-label incorporation

Chl *a* was extracted from plants grown in half-strength Hunter's medium (labeled sample) supplemented with labeled ALA and from unlabeled plants (reference sample), according to the following procedure (Moran and Porath 1980): Plants were homogenized in half-strength Hunter's medium and centrifuged for 10 min at 16000 × *g*. The supernatant was removed and the residue was dissolved in 1 ml MeOH. The methanolic solution was centrifuged for 5 min at 300 × *g*. The green supernatant was separated from the blue and white residue and dried under a gentle stream of N_2. The sample was resuspended in acetone, loaded on a cellulose column and pure Chl *a* fractions were eluted with petroleum

ether/acetone (7/3 v/v). The solvent was evaporated under N_2 flow and the pure Chl *a* was stored at -20 °C in a dry nitrogen atmosphere.

Mass spectra were measured with a Linear Trap Quadrupole Forier Transform (LTQ–FT) hybrid mass spectrometer (Thermo Fisher Waltham, MA, USA). Spectra were measured in the ESI mode, with a source temperature of 200°C, a source voltage of 3.8 kV and a tube lens voltage of 150 V. Chl *a* was dissolved in 90% EtOH and 10% 10 mM ammonium acetate to a final concentration of ~1 mg/mL. The sample was infused with a flow rate of 10 $\mu Lmin^{-1}$. In the biosynthetic route from ALA to Chl *a* and Phe *a*, two molecules of 5-, 4-, or 3-ALA are asymmetrically condensed to form the pyrrole porphobilinogen (PBG). Four molecules of PBG tetramerize, and prior to macrocycle ring closure, the last pyrrole ring is inverted via a spiro-intermediate (Schulten *et al.* 2002). Upon incorporation of 5-, 4-, or 3-ALA a maximum of 8 ^{13}C can be incorporated into each Chl *a* or Phe *a* molecule, which leads to the sparse labeling patterns shown in Figure A1 in Appendix 1. Based on the LC-MS spectra observed in the region of m/z = 893.5 ([M]•+; $C_{55}H_{72}O_5N_4Mg$) to m/z +8 (maximum ^{13}C incorporation) the total level of incorporation (P_{tot}) was determined via an iterative procedure as described earlier by Schulten *et al.* (Schulten *et al.* 2002) and in section 2.3.1 of this thesis. Since ALA is a precursor of both Chl *a* and Phe *a*, it is assumed that the level of label incorporation into Phe *a* and Chl *a* is identical (Beale and Weinstein 1991). Figure A1 shows a characteristic mass spectrum of Chl *a* isolated from *S. oligorrhiza* grown under standard conditions (see Appendix A, Figure A1 and Table A2) and in the presence of ^{13}C labeled ALA precursor (Figure A1B). An average of 30% isotope enrichment was accomplished.

4.2.3 Isolation of PSII D1D2, BBY and Core complex

The natural abundance samples of isolated D1D2 from spinach were prepared as described earlier in Matysik *et al*. (Matysik 2000) The PSII core complexes from duckweed were isolated according to the procedures described by van Leeuwen *et al*. (van Leeuwen *et al.* 1991)

Selectively ^{13}C labeled BBY membranes were isolated according to the methods described in (Berthold *et al.* 1981). This procedure was adjusted for micro scale preparation using 10 g of 4-ALA labeled duckweed plants as a starting material. After solubilization in MES buffer (20 mM MES, 15 mM $NaCl_2$, 5 mM $MgCl_2$, pH 6.0), starch was removed by 5

minutes of slow centrifugation (Sorvall SS34) at 80 × *g*. The Chl *a* concentration of the reaction mixture was determined using a Moran Assay and adjusted to 1 mg/mL. Triton-100 was added to a final concentration of 5% (w/v). After incubation on ice while stirring for 20 minutes the sample was centrifuged for 20 minutes at 25,000 × *g*. The pellet was resuspended in MES buffer to remove the Triton-100 and again centrifuged for 20 minutes at 25,000 × *g*. The product, 1.5 mL of 1.7 mg/mL Chl *a*, was stored at -80°C in BTS-200 buffer (20 mM Tricine, 10 mM $MgCl_2$, 5 mM $CaCl_2$,10 mM $MgSO_4$, 0.2 M Sucrose and 0.03% (w/v) n-dodecyl-β-D-maltoside, pH 6.5).

4.2.4 NMR sample preparation

D1D2 was directly loaded into an optically transparent 4-mm NMR sapphire rotor. All other samples were previously reduced by the addition of sodium dithionite to a final concentration of 100 mM under oxygen free and low light conditions and loaded into NMR sapphire rotors. For experiments on BBY, 200 µL of BBY product (Chl *a* concentration of 1.7 mg/mL) was washed twice with sucrose free BTS-200 buffer (BTS-0) and resuspended in 70 µL of BTS-0 before reduction. For preparation of thylakoid samples ~200 mg isotope labeled plants were homogenized in a minimal amount of half-strength Hunter's medium at pH 5.8 under near dark conditions. Starch was removed with slow centrifugation at 60 × *g* for 3 minutes (Eppendorf 5415D). The supernatant was collected and centrifuged for 10 min at 16000 × *g*, and the pellet was resuspended in half strength Hunters medium. For experiments on entire plants, ~100 mg duckweed plants was incubated for 15 minutes in a solution containing 100 mM sodium dithionite in complete darkness in a nitrogen atmosphere. Plants were carefully stacked inside an optically transparent 4-mm NMR sapphire rotor and half-strength Hunter's medium was added to fill the rotor. In all cases the filled rotor was directly loaded into the NMR-probe and cooled to 235 K with slow sample spinning at 800 Hz.

For a high triplet yield and subsequent photo-CIDNP buildup it is necessary to doubly reduce the quinones (Q, Figure 4.1C). Only in D1D2 preparations reduction is not required because the quinones are already lost during D1D2 preparation. Double reduction of both Q_A and Q_B was realized by the addition of sodium dithionite to a final concentration of 100 µM. Membrane and plant samples were always freshly prepared and directly frozen inside the NMR apparatus.

4.2.5 Photo-CIDNP MAS NMR experiments and data processing

^{13}C-MAS NMR experiments were performed with a DMX-200 NMR spectrometer (Bruker Biospin GmbH, Karlsruhe, Germany). All spectra have been obtained at a sample temperature of 235 K and with a spinning frequency of 8 kHz. The spectra were collected with a spin echo pulse sequence with phase cycling of (π/2) pulses under two-pulse phase modulation carbon-proton decoupling (Bennett *et al*.). Photo-CIDNP MAS NMR spectra have been obtained using continuous illumination with a 1000-Watt Xenon arc lamp (Matysik *et al.* 2000).

The fitting of the light induced signals obtained by MAS NMR photo-CIDNP has been performed using Igor Pro version 6.01 (Lake Oswego, Oregon).

4.3 RESULTS AND DISCUSSION

4.3.1 Comparison of ^{13}C Photo-CIDNP MAS NMR spectra of isolated PSII systems from spinach and duckweed.

In Figure 4.4A, Spectra a and b were obtained by continuous illumination of D1D2 from spinach and core particles from unlabeled duckweed. Spectra a′ and b′ show the corresponding dark spectra. The dark spectra show signals in the aliphatic region between 0 and 50 ppm, as well as a broad signal between 60 and 80 ppm. These dark signals are due to the C-α of the amino acids of the protein backbone. In the photo-CIDNP spectra in Figure 4.4A (a,b), absorptive (positive) light-induced signals occur in the region between 120 and 170 ppm. These signals have been assigned to the aromatic ring carbons of the Chl *a* donor based on our previous study (Diller *et al.* 2005) (Table 4.1). Emissive signals between 90 and 130 ppm were identified as four methine carbons. Figure 4.4B shows the aromatic regions of Spectra a and b in Figure 4.4A. A total of 23 light-induced signals previously assigned to the Chl *a* donor (Table 4.1) are visualized by dashed lines. The broad negative response observed at 142.5 and 146 ppm and the emissive signal at 129.2 ppm can be sttributed to a response from aromatic amino acids in the vicinity of the Chl *a* donor (Diller *et al.* 2005; Holzwarth *et al.* 2006).

The photo-CIDNP signals obtained by illumination of a spinach D1D2 preparation (a) and duckweed PSII core particles (b) are similar, both with respect to the chemical shifts and in terms of the overall intensity pattern. These data corroborate earlier work by

femtosecond transient absorption spectroscopy, which revealed a conservation of the efficient electron transfer rate constants upon isolation of the D1D2 complex from PSII core (Holzwarth *et al.* 2006). Also the mechanism of electron transfer, with Chl_{D1} acting as the primary electron donor and Phe_{D1} as the primary acceptor, was found to be the same in both D1D2 and PSII core systems (Holzwarth *et al.* 2006).

The data obtained from the core complex show a lower signal to noise ratio compared to data obtained from the fully isolated system, due to less PSII RCs per unit area in PSII core complex preparations, compared to isolated RCs. A ratio ~1:5 is estimated based on the 80% drop in relative OD_{675} absorption upon isolation of D1D2 from PSII core. Based on these numbers and the observation of a single Chl component with narrow signals, the presence of different RC subpopulations or a substantial inactive PSII fraction is highly unlikely. For the preparation of both the D1D2 and PS2 core, treatment with Triton-X detergent is used (Leeuwen *et al.* 1991). Triton-X has been found to affect the absorption and hole burning spectra of PSII, disrupting the charge transfer from the Chl_{D1} to Phe_{D1} in the first picoseconds after excitation (Tang *et al.* 1991). In addition it has been suggested that D1D2 preparations contain two subpopulations of fully intact and destabilized (blue shifted) PSII with a distorted P_{D1}-P_{D2} coupling (Hillmann *et al.* 1995; Riley *et al.* 2004; Acharya *et al.* 2012).

In the current work the PS2 core complex is studied when embedded in its natural membrane environment, in the thylakoid membrane. Observation of photo-CIDNP from thylakoid membranes is difficult without the additional sensitivity that can be obtained by specific isotope labeling. To compare the radical-pair structure of PSII in isolated D1D2 particles with that of PSII embedded in native thylakoid membrane or in intact leaves, site specific ^{13}C labeling in Chl *a* and Phe *a* of PSII in duckweed were performed.

4.3.2 Observation of ^{13}C photo-CIDNP from site-specific ^{13}C labeled PSII in native thylakoid membrane

Figure 4.4C shows ^{13}C photo-CIDNP spectra from PSII in native thylakoid membrane from duckweed plants that were specifically ^{13}C labeled at different carbon positions by feeding plants with ^{13}C labeled precursors of chlorophylls. The isotope label patterns for the Chl *a* donor and Phe *a* acceptor, obtained by feeding with ^{13}C 5-ALA, 4-ALA and 3-ALA are indicated in Figure 4.3. By using specifically labeled samples it was

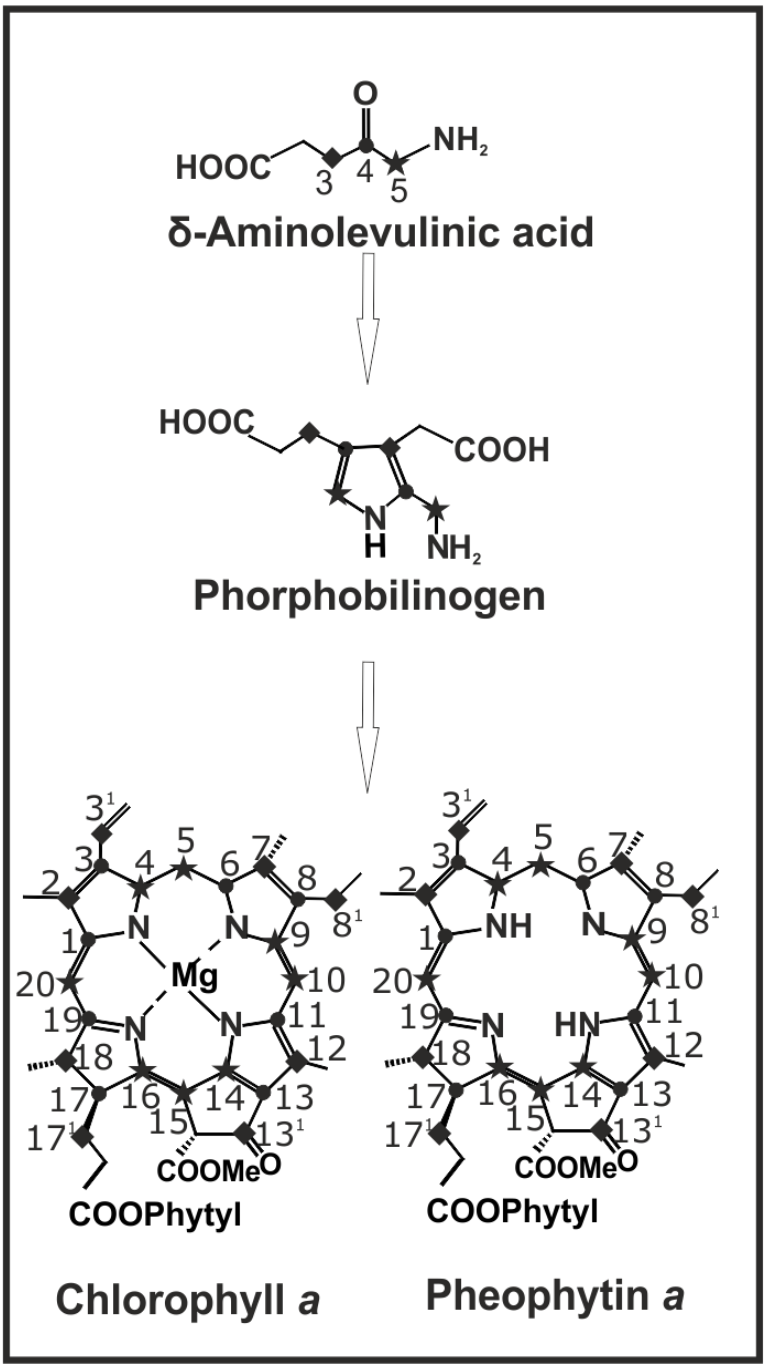

Figure 4.3: Incorporation of ^{13}C labels by feeding 5-aminolevulinic acid (ALA), 4-ALA or 3-ALA precursors to the growing plants. Depending on the placement of the ^{13}C isotope within the precursor (at position 5, 4 or 3) the Chl *a* and Phe *a* molecules are labeled during the natural biosynthesis pathway at the positions visualized by the different symbols. With the stars, circles and diamonds referring to the pattern obtained by the addition of 5-, 4- or 3-ALA precursors, respectively. The numbering of Chl *a* and Phe *a* is according to the IUPAC nomenclature.

possible to selectively highlight eight carbons in each active Chl *a* or Phe *a* cofactor (Figure 4.3).

From the 23 light induced signals obtained from unlabeled PSII core and D1D2 systems (Figure 4.4B), 19 signals can be traced back in the data obtained from selectively

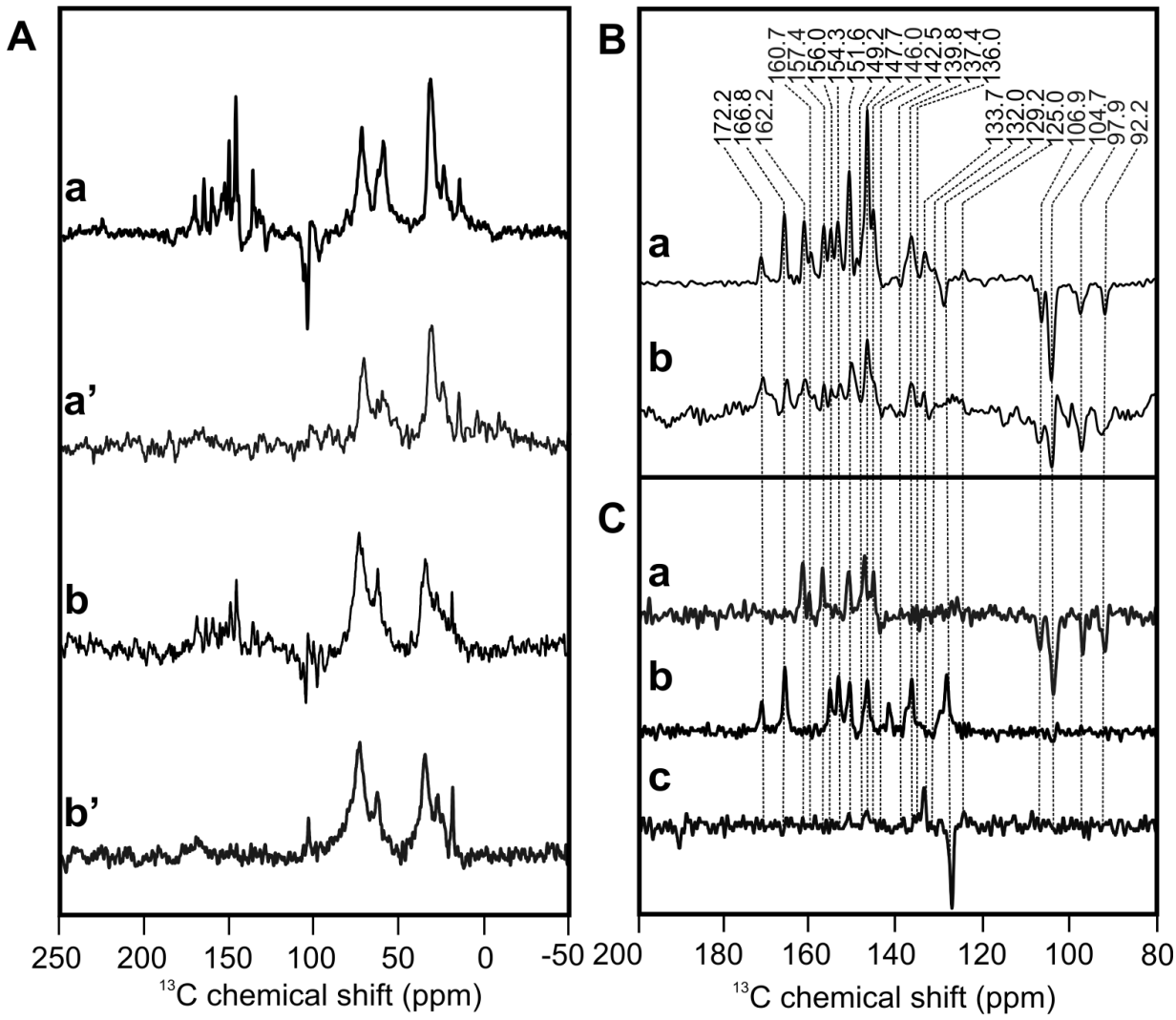

Figure 4.4: (A) ^{13}C photo-CIDNP MAS NMR spectra obtained by continuous illumination of D1D2 particles of spinach with ^{13}C at natural abundance (a) and unlabeled core complexes of duckweed (b). Spectra a′ and b′ depict the corresponding spectra obtained in the dark. (B) Aromatic region of the continuous illumination spectra of Figure 4.3A. (C) ^{13}C photo-CIDNP spectra from PSII in native thylakoid membrane from duckweed plants labeled with ^{13}C 5-ALA (a), 4-ALA (b) or 3-ALA (c).

labeled thylakoid membranes (Figure 4.4C). Upon comparison of the spectrum obtained from unlabeled isolated PSII (Figure 4.4B) with data collected from selectively labeled thylakoid membranes (Figure 4.4C) a remarkable conservation of the relative signal intensities emerges, if the signal overlap at 129.2, 147.7 and 151.6 ppm is taken into account. The chemical shift pattern is the same for the various samples. This clearly demonstrates the conservation of the electronic structure of the PSII Chl *a* donor upon isolation of core particles from thylakoid membranes.

In Table 4.1, the ^{13}C chemical shifts of the photo-CIDNP signals obtained from selectively ^{13}C-labeled thylakoid membranes from duckweed are compared with the signals observed for D1D2 samples of spinach with ^{13}C at natural abundance, literature values of

Table 4.1: ^{13}C chemical shifts of the photo-CIDNP signals of sparsely ^{13}C-labeled PSII embedded in thylakoid membranes from duckweed in comparison with literature data for unlabeled isolated spinach D1D2 and solid state NMR chemical shifts of Chl *a* and Phe *a* molecules or aggregates.

Chl *a*	Phe *a*	Carbon atom	PSII D1D2	PSII Thylakoid
σ_{ss} [a]	σ_{ss} [b]		σ_{ss} [c]	σ_{ss} [d]
190.6	190	13[1]		190.4 e
170.0	171	19	166.8 a 172.2 a	166.6 a 171.9 e
162.0	151	14	162.2 a 151.6 a	162.1 a 151.5 a
155.9	142	1	156.0 a 142.5 e	156.0 a 142.3 a
154.4	156	6	154.3 a	155.0 a 153.9 a
154.0	161	16	157.4 a 160.7 a	157.5 a 160.6 a
150.7	137	4	149.2 a	148.8 a 145.7 a
147.2	138	11	147.7 a	147.2 a
147.2	150	9	146.0 a	147.8 a 146.6 a
146.2	145	8		151.4 a 148.1 a
138.0	136	3	139.8 e 137.4 a	138.2 a 136.9 a
136.1	131	2	136.0 a	-
134.0	128	12	133.9 a	134.2 a?
133.4	136	7	~ 132 a	-
126.2	133	13		130.2 a 128.8 a
126.2	129	3[1]	~ 125 a	127.8 e 124.7 a
108.2	105	10	106.9 e	107.2 e
102.8	107	15	104.7 e	103.9 e 104.8 e
98.1	97	5	97.9 e	97.9 e
93.3	93	20	92.2 e	93.0 e 92.0 e
51.4	52	17		48.9 a 51.0 a
32.5	32	17[1]		29.3 a
20.2	19.8	8[1]		19.6 a

[a] Boender (1995), data obtained from solid aggregates of Chl a (Boender *et al.* 1995).

[b] Egorova (1997) solid state data obtained from plant pheophytin a recomstituted in *Rb. sphaeroides* R26 RCs (Egorova Zachernyuk *et al.* 1997).

[c] Diller et al. (2005), data obtained from D1D2 particles of spinach (Diller *et al.* 2005).

[d] This work, solid state data obtained from specifically labeled thylakoid membranes of duckweed. Abbreviations: σ_{ss} = solid state chemical shift in ppm, a = absorptive signal, e = emissive signal.

signals obtained from Chl *a* aggregates (Boender *et al.* 1995) and the response from plant Phe *a* reconstituted in bacterial RCs (Egorova-Zachernyuk *et al.* 2008). Although all the Chl *a* and Phe *a* molecules that are present in the samples contain 5-, 4- or 3-ALA labeled cofactors, only carbons from cofactors forming the primary radical pair are expected to be enhanced upon illumination due to the solid-state photo-CIDNP effect. The ^{13}C-^{13}C spin diffusion between nearby isotope labels on the same cofactor allows for some equilibration of intensities of signals originating from labeled carbons in direct vicinity of each other (Matysik *et al.* 2001; Daviso *et al.* 2009).

In the spectrum obtained from 5-ALA labeled thylakoid samples, 14 light induced signals can be resolved. Based on a comparison with chemical shifts obtained from solid state data for aggregated Chl *a*, and Phe *a* reconstituted in *Rb*. *sphaeroides* RCs (Egorova-Zachernyuk *et al.* 2008), eight of the 14 signals can be assigned to the Chl *a* donor and 6 to the Phe *a* acceptor. The emissive signals between 90 and 130 ppm, which were assigned previously to the four methine carbons (Matysik 2000; Diller *et al.* 2005), appear in the spectrum obtained from 5-ALA labeled PSII (Figure 4.4C). Hence, the assignment based on selective isotope labelling contribute to converging and convincing evidence from MAS NMR photo-CIDNP studies for a monomeric donor and a monomeric acceptor forming the radical pair (Matysik 2000; Diller *et al.* 2005).

The spectrum obtained from 4-ALA labeled thylakoid membrane preparations shows 15 light-induced signals. Based on a comparison with chemical shifts obtained from solid state data of aggregated Chl *a* (Boender *et al.* 1995), eight of the 15 signals can be attributed to the Chl *a* donor. Interestingly, similar to the 5-ALA spectrum, the eight signals of the Chl *a* donor, in general, are stronger than the remaining seven. Based on their chemical shifts, the remaining seven are tentatively assigned to the Phe *a* acceptor (Egorova-Zachernyuk *et al.* 2008). The C-19 carbonyl of the Chl *a* donor is at rather high field of 166.6 ppm suggesting some local interaction (Diller *et al.* 2005).

The spectrum obtained from 3-ALA labeled thylakoid, which has the ^{13}C labels mostly positioned on aliphatic carbons (Figure 4.3), shows a limited number of light-induced signals compared to the data collected from the 5- and 4-ALA preparations with the ^{13}C isotopes in the macroaromatic cycle. Based on the literature data the strong emissive signal at 128.7 ppm is assigned to the C-3^1 of the Phe *a* acceptor, while the much weaker absorptive 124.7 ppm is assigned to the corresponding C-3^1 of the Chl *a* donor (See Table 4.1 and Figure 4.4 green trace; Boender *et al.* 1995; Egorova-Zachernyuk *et al.* 2008). The emissive

signal at 190.4 ppm is assigned to the C-13^1 carbonyl of the Chl *a* donor. This shift essentially rules out the possibility of the protonation of the C-13^1 carbonyl group in P_{D1} Chl *a* (Matysik 2000) as the possible source of an electric field polarizing the donor. In addition, since the chemical shift is close to the value observed for monomeric Chl *a*, a local chemical perturbation at this carbonyl is unlikely. The absorptive signal at 134.2 ppm is tentatively assigned to the C-12 of the Chl *a* donor and two weak absorptive features at 29.3 and 19.6 ppm (data not shown) match with the ^{13}C-17^1 and ^{13}C-8^1 responses observed for the models.

4.3.3 The involvement of the protein backbone and possible alternative electron spin carriers:

Two weak emissive signals at 142.5 and 139.8 ppm and two absorptive signals at 136.0 and 132.0 ppm that are observed in the spectra for the unlabeled PSII (Figure 4.4B) did not appear in the spectra obtained from PSII in thylakoid membrane that was sparsely ^{13}C labeled in the Chl *a* and Phe *a* and embedded in the thylakoid membrane (Figure 4.4C). While for the unlabeled species all carbons participating in primary charge separation events and carrying electron spin density can be observed by photo-CIDNP, the biosynthetic incorporation of ^{13}C highlights only the carbons of the Chl *a* and Phe *a* pigments, that are adressed by the labeling pathways. All carbons within the aromatic ring, C-1 to C-20, the C-13^1 carbonyl and the aliphatic carbons C-3^1, C-8^1 and C-17^1 are highlighted in either the 3-, 4- or 5-ALA ^{13}C-labeled preparations. The remaining aliphatic carbons of the Chl *a* and Phe *a* cofactors are not expected to carry electron spin density and, according to previous assignments, are not expected to resonate at the frequencies of the additional signals that are observed at 142.5, 139.8, 136.0 and 132.0 ppm. (Boender *et al.* 1995; Egorova-Zachernyuk *et al.* 2008). Therefore, our data strongly suggest that some electron spin density is attached to an amino acid, in addition to the electron spin density that is localized on the Chl *a* and Phe *a* cofactors.

The presence of the signals at 136.0 and 132.0 ppm in the unlabeled samples compared with the response from the set of labeled samples supports the proposal for a spin carrying histidine residue in close proximity of the Chl *a* donor P_{D1} (Matysik *et al.* 2001; Diller *et al.* 2005). Recently it has been suggested that a Chl$^{\delta-}$-His$^{\delta+}$ partial charge transfer motif is a common denominator across photosynthetic RC complexes in plants and bacteria and that this interaction lowers the energy barrier in photosynthetic complexes (Alia *et al.*

2013; Matysik *et al.* 2001; Alia *et al.* 2009). Experiments with selectively ^{15}N-ALA label patterns would be of great interest to arrive at a final conclusion regarding the involvement of electron spin carriers on the protein backbone (See chapter 6 for preliminary results).

It has been suggested that the emissive features at 139.8 and 142.5 ppm can be associated with a Schiff base or a carotenoid molecule (Diller *et al.* 2005, Breitmai and Voelter 1990). However, in contrast with bacterial systems, the carotenoids in PSII are not active as triplet quenchers when Q_A is doubly reduced or absent. If Q_A is singly reduced the carotenoid associated with the D_2 branch ($Car_{D2,}$ see Figure 4.1C) can act as a fast triplet quencher (Martinez-Junza *et al.* 2008). Possibly, a fraction of the PSII in our experiments remains in the singly reduced state providing the possibility for ρ_i buildup and quenching on the carotenoid.

4.3.4 Comparison of the data obtained from labeled BBY, Thylakoids and Plants:

Figure 4.5A compares the photo-CIDNP spectra from BBY (a), thylakoid membranes (b), and from entire plants (c) of selectively 4-ALA ^{13}C-isotope labeled duckweed. Figure 4.4B shows a detailed view of the light-induced spectra of Figure 4.5A. A total of 15 light induced signals can be distinguished and a comprehensive assignment of the Chl *a* donor and Phe *a* acceptor was deduced from the combination of spectra obtained from the sparsely labelled samples (Table 4.1). The pattern of isotope labels for the Chl *a* donor and Phe *a* acceptor, obtained by feeding with ^{13}C 4-ALA, is indicated by the black dots that are shown in the inset in Figure 4.5B. Interestingly, the comparison of the photo-CIDNP spectra of BBY particles, thylakoid membrane and intact leaves did not reveal any significant change. Minor changes in the relative intensities of the signals shifted to 51.0 and 147.2 ppm are observed. These can be attributed to a difference in concentration of RCs in various samples, which is, for example, limited by the small number of plants that fit inside the MAS NMR rotor. Hence both the chemical shifts and the overall intensity pattern are highly conserved among spectra obtained from BBY (spectrum 4.5a), thylakoid (spectrum 4.5b) and plant (spectrum 4.5c), demonstrating that the inner photochemical machinery forming the primary radical pair remains essentially unaffected upon extraction of thylakoid membrane from the plants and upon extraction of PSI from the thylakoid membrane, *e.g.* BBY isolation.

The dark spectra collected from BBY (spectrum a′), thylakoids (spectrum b′) or entire plants (spectrum c′) are very similar (Figure 4.5). The dark spectra show only a very weak

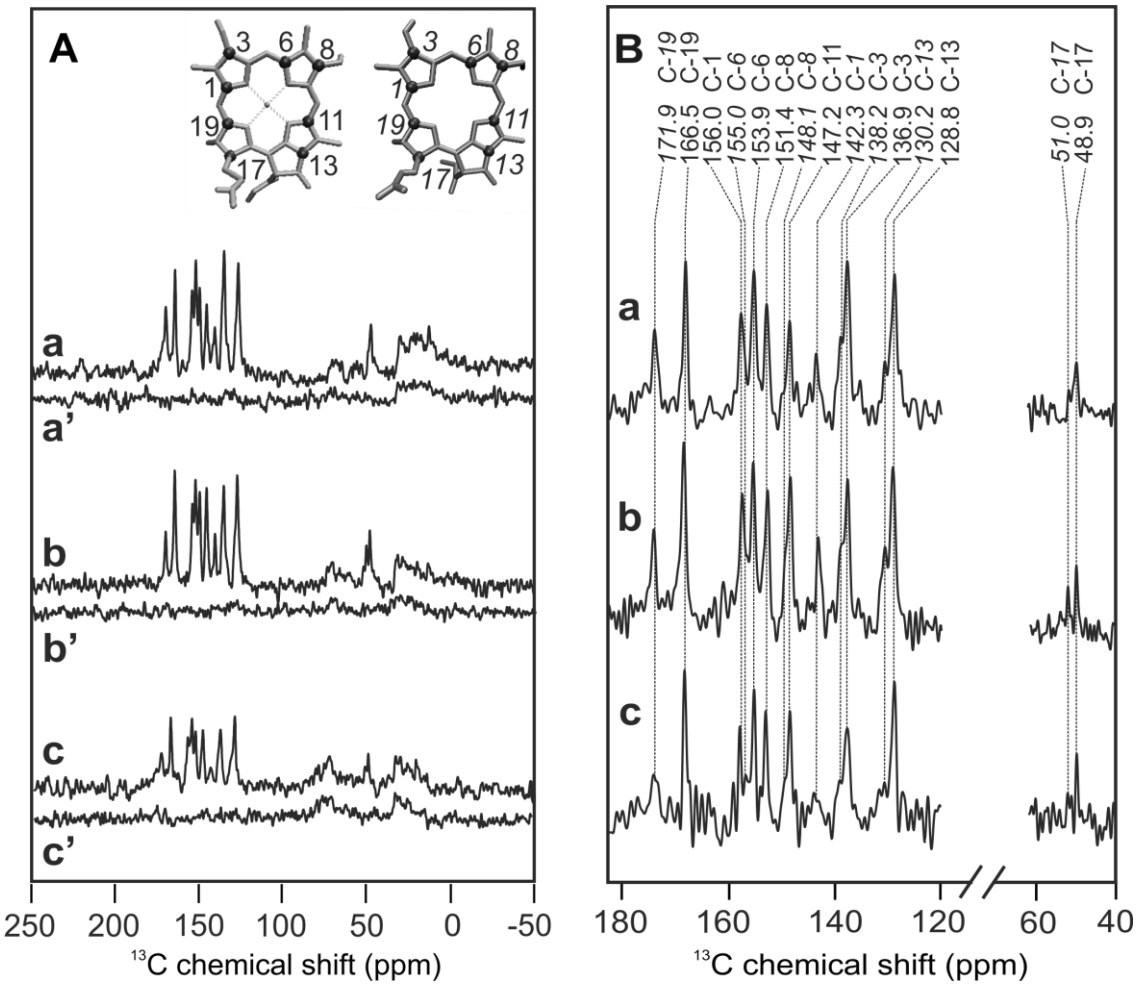

Figure 4.5: ^{13}C photo-CIDNP MAS NMR spectra obtained by continuous illumination of BBY (a) thylakoid membrane (b) and entire plants (c) obtained from selectively 4-ALA ^{13}C-isotope labeled duckweed. Spectra a′, b′ and c′ show the corresponding spectra obtained at dark conditions. B shows the signals occurring in the aromatic and aliphatic regions of the photo-CIDNP MAS NMR spectra. The Chl *a* donor (left) and the Phe *a* acceptor (right) with the positions of the ^{13}C-isotope labeled carbons (black dots) are depicted in upper right corner. The numbering follows the IUPAC nomenclature. Assigned centerbands are visualized by dashed lines. Signals assigned to the Phe *a* acceptor are written in italic.

broad positive signal in the aliphatic region between 0 and 50 ppm and between 60 and 80 ppm from to the ^{13}C-α nuclei at natural abundance in the the amino acids of the protein backbone, which matches the response from the unlabeled samples.

The data provide clear evidence for the same pattern of chemical shifts as well as photo-CIDNP intensities in the light-induced spectra of BBY, thylakoids and plants. Hence we conclude that the inner photochemical machinery is not modified or damaged by any of these isolation steps. While thylakoid and plant samples contain the full photosynthetic machinery, including both PSII and PSI, BBY contains PSII only. While the apparent absence of photochemically active PSI (Alia *et al.* 2004), can be due to several reasons, probably a selective reduction of quinone is most relevant. The quinones on PSII are easily

accessible and instantaneously reduced upon addition of sodium dithionite, which contrasts with the quinones in PSI that are difficult to reduce upon direct freezing and measurement (Feldman *et al.* 2007). To successfully reduce PSI, incubation at room temperature after addition of the reductant, and exposure to light at room temperature and during freezing are necessary (Janssen *et al.* 2010). In addition the pH of the sample environment favours observation of the photo-CIDNP effect in PSII. In *vivo* the active site of PSI is located at the alkaline stroma side of the thylakoid membrane that is in an alkaline environment with pH 8, while PSII functions at the acidic lumen side of the membrane with pH ~4.5 (Anderson *et al.* 2008). Acidic conditions strongly decrease PSI stability and activity (Yang *et al.* 2009) while the donor/acceptor side of PSII is known to remain intact under strong acidic conditions (Mathur *et al.* 2011). In any case, destructive interference of the emissive signals from PSI by the stronger absorptive signals of Chl *a* from PSII in the spectra of thylakoid membranes and plants is very unlikely due to the similarity between the data for the thylakoid preparations and the spectrum collected from BBY particles.

4.3.5 Photo-CIDNP buildup in BBY, Thylakoids and Plants

Since the OEC and the Tyr_Z are oxidized by hole transfer from the P680, the generation of a $P_{D1}^{+}Phe^{-}$ radical pair with sufficient lifetime to produce photo-CIDNP, *i.e.*, some ~10-100 ns, is an experimental challenge (Blankenship *et al.* 1975). In particular for larger PSII systems both the secondary electron acceptor Q_A and the OEC can become active and the electron transfer steps (e_2 to e_4) from the ($P_{D1}^{+}Phe^{-}$) radical pair can quench the photo-CIDNP effect (see Figure 4.2, page 66). The photo-CIDNP results presented here demonstrate that in higher preparations with the OEC the same radical species is present as for the D1D2 preparation without the OEC. The addition of $Na_2S_2O_3$ reductant lowers the pH and leads to slow electron transfer from the OEC to P_{D1}^{+} for higher sample preparations, thereby confining the radical pair for photo-CIDNP buildup. Previous studies have shown that the rate of re-reduction of P_{D1}^{+} (by Tyr_Z) decreases at low pH (Pulles *et al.* 1976). This was attributed to a distortion or breakage of the hydrogen bond between Tyr_Z and the nearby D1-His190, which has an estimated pKa of 4.5-5.3 (Rautter *et al.* 1995) (for a review see Styring *et al.* 2012). Such acidification of the lumen space down to a pH of 5.0 or slightly below also occurs *in vivo* under strong light conditions (Graber and Witt 1976). The pH dependence provides a natural mechanism for physiological regulation of electron transfer from the OEC, allowing for dissipation of excess excitation energy by the RC at high-light

conditions (Rochaix 2011). According to the Kok model, the mechanism for water oxidation is described by the S-cycle (Gorkom and Schelvis 1993). Here S0 to S4 refer to the intermediate redox states in the OEC and S1 is the state that is stable in the dark. After the oxidation of two water molecules and formation of an O-O bond, O_2 is released and the OEC returns from the S4 to the S0 state. The S-cycle is enabled for T > 250K and is strongly inhibited at ~ T = 230K (Styring and Rutherford 1988). In the temperature region of our experiment *T* ~ 235K, the S1 to S2 transition is allowed while the step to S3 and beyond is blocked. At low pH (<5.0) strong inhibition of the S2 to S3 transition occurs at T < 283K (Bernat *et al.* 2002; Suzuki *et al.* 2005). Hence with the experimental conditions employed in the current study the S2 intermediate of the OEC will most probably accumulate. When the OEC converts from the S1 to the S2 state, the reduction rate of P_{D1} slows down from 50 ns to 250 ns at pH 6-7.5 (Rappaport *et al.* 1994).

On the other side of the electron conversion chain, linear electron flow under natural conditions proceeds via the electron transfer step e_2 in Figure 4.2. This leads to depletion of the P_{D1}-Phe *a* radical pair state on a time scale of ~300 ps, which is very short compared to the time scale of the coherent buildup of the photo-CIDNP signal. Hence, for the fraction of the radical pairs that produce the light-induced nuclear polarization, the downstream electron transfer from the Phe *a* is blocked or slowed down considerably at the Q_A acceptor site. For D1D2 preparations quinone removal blocks the electron transfer and leads to radical pairs with sufficient long lifetimes for photo-CIDNP. In core preparations, however, Q_B is lost while Q_A remains bound to the protein pocket (Ghanotakis *et al.* 1987). In higher preparations, both quinones are, at least initially, present. Most likely the Q_B is lost upon reduction prior to the measurement.

To block the downstream electron transfer in core and higher preparations, double reduction of Q_A is necessary. It has been shown to occur under natural conditions at high light intensities, and leads to the release of up to 63% Q_A as Q_AH_2 in 80 min (Koivuniemi *et al.* 1993)). For core preparations, double reduction of Q_A can be significantly enhanced by the addition of a strong reductant and subsequent illumination (Feikema *et al.* 2005; Cox *et al.* 2009). In BBY preparations, illumination for ~10 min followed by 25 min of dark adaptation under reductive conditions at 40 mM sodium dithionite and 100 mM benzylviologen leads to 100% double reduction of Q_A (van Mieghem *et al.* 1995). In their early photo-CIDNP studies on RCs of *Rb. sphaeroides* R26, Zysmilich and McDermott reported significant and characteristic differences between the responses from Q-reduced and

Q-depleted samples (Zysmilich and McDermott 1996). In the photo-CIDNP data collected from PSII, the spectra for D1D2 and core preparations are very similar, which is in line with the converging evidence that Q_A is lost in reduced core preparations. Double reduction and release of Q_A is, in contrast to the release of reduced Q_B, irreversible, since it induces a change in the Q_A protein binding pocket (Vass *et al.* 1992). If oxygen is present, the blocking of ET by the absence of oxidized ('open') Q_A leads to the formation of singlet oxygen species and fast degradation of the D1 protein (minutes at room temperature) (Frank *et al.* 1989; Breitmai.E and Voelter 1990; Durrant *et al.* 1990; Vass *et al.* 1992; Ishikita *et al.* 2005). Under anaerobic conditions double reduction of Q_A increases the radical-pair lifetime from 20 to 250 ns which results in a high triplet yield (Frank *et al.* 1989; Lubitz *et al.* 2002) allowing photo-CIDNP build-up.

Recent data obtained by femtosecond transient absorption studies and theoretical calculations (Novoderezhkin *et al.* 2005; Holzwarth *et al.* 2006; Raszewski *et al.* 2008; Novoderezhkin *et al.* 2011) indicate a coexistence of at least two ET channels at early stages of charge separation (< 20 ns), with a single $P^+_{D1}Phe^-_{D1}$ species at later stages of the photochemistry. Our data reveal a homogeneous steady state at longer time scales. A partial or complete conversion into a photochemically active P^+_{D2} species that could not be excluded by the optical work (Raszewski *et al.* 2008) is unlikely in the steady state observed with photo-CIDNP. Specific shaping of the P_{D2} by the protein environment makes that a correlated radical pair state involving the P^+_{D2} is expected to give rise to a photo-CIDNP signal component with chemical shifts that are different from the P^+_{D1} and hence to signal doubling, while in all the CIDNP data collected from different PSII preparations the same and unique Chl *a* response is observed.

4.3.6 Conclusions

Here we demonstrate that the solid-state photo-CIDNP effect in conjunction with selective isotope incorporation allows for observation of NMR signals, of primary radical pair of PSII, directly from thylakoid membranes as well as from the entire plants (Figure 4.6). At the atomic resolution, it is demonstrated that the active photochemical machinery forming the primary radical pair of PSII is conserved between different higher plant species. In addition our results show that the photochemical machinery is remarkably robust and remains essentially unaffected by the various preparation procedures, since there are very

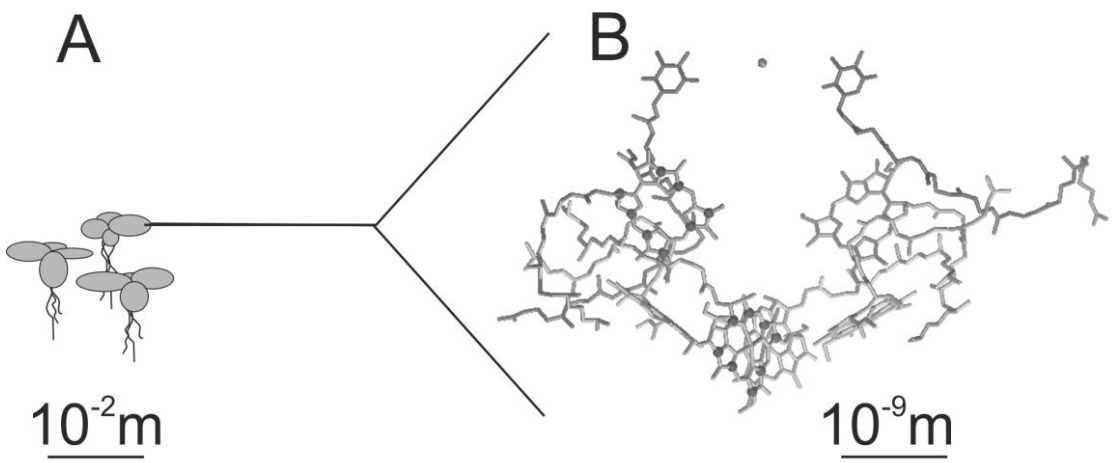

Figure 4.6: By combining specific isotope labeling with the photo-CIDNP technique signals from carbon atoms at labeled positions (B, dark grey balls) within the active Chl *a* and Phe *a* cofactors can be detected and it is possible to cover a range from the macroscopic plant scale of duckweed leaves (A) to the atomic scale of the PSII RC (B). The average adult leaf size of duckweed is 4 mm in length making it suitable to fit in an optically transparent 4-mm sapphire MAS NMR rotor.

little changes in the photo-CIDNP response across sample preparations from plant level to the D1D2 preparation. The data establish that the radical pair is clearly formed by a single Chl *a* and a single Phe *a*. In addition, there is significant empirical evidence for the involvement of the protein matrix. These observations can be explained by assuming the involvement of a histidine carrying a part of the electron spin density. In this chapter an explanation for the mechanism of photo-CIDNP buildup in larger PSII systems has been presented. The observation of photo-CIDNP MAS NMR directly from plants allows future application of this method for testing of the occurrence of radical pairs and the analysis of these in systems in which a further isolation has not yet been established or is too expensive.